Published in final edited form as:
Clin Chem. 2013 June ; 59(6): 949–958. doi:10.1373/clinchem.2012.196949.

A Comparison of the Theoretical Relationship between HDL Size and the Ratio of HDL Cholesterol to Apolipoprotein A-I with Experimental Results from the Women's Health Study

Norman A. Mazer[1], **Franco Giulianini**[2], **Nina P. Paynter**[2], **Paul Jordan**[3], and **Samia Mora**[2,4]

[1]Clinical Pharmacology, F. Hoffmann - La Roche, Basel, Switzerland [3]Biostatistics, F. Hoffmann - La Roche, Basel, Switzerland [2]Division of Preventive Medicine, Brigham and Women's Hospital, Boston, MA, USA [4]Division of Cardiovascular Medicine, Brigham and Women's Hospital/Harvard Medical School, Boston, MA, USA

Abstract

Background—HDL size and composition vary among individuals and may be associated with cardiovascular disease and diabetes. We investigated the theoretical relationship between HDL size and composition using an updated version of the spherical model of lipoprotein structure proposed by Shen et al. and compared its predictions with experimental data from the Women's Health Study (WHS).

Methods—The Shen model was updated to predict the relationship between HDL diameter and the ratio of HDL-cholesterol (HDL-C) to apolipoprotein A-I (ApoA-I) plasma concentrations, i.e., the HDL-C/ApoA-I ratio. In WHS (n=26,772), NMR spectroscopy was used to measure the average HDL diameter ($d_{avg,NMR}$) and particle concentration (HDL-P); HDL-C and ApoA-I (mg/dL) were measured by standardized assays.

Results—The updated Shen model predicts a quasi-linear increase of HDL diameter with the HDL-C/ApoA-I ratio, consistent with the measured $d_{avg,NMR}$ values from WHS, which ranged between 8.0 and 10.8 nm and correlated positively with the HDL-C/ApoA-I ratio (r=0.608, $p<2.2\times10^{-16}$). The WHS data were further described by a linear regression equation: d_{WHS} (nm) = 4.66 + 12.31 HDL-C/ApoA-I. The validity of this equation for estimating HDL size was assessed with data from CETP deficiency and pharmacologic inhibition. We also illustrate how HDL-P can be estimated from the HDL size and ApoA-I level.

Conclusions—This study provides a large-scale experimental examination of the updated Shen model, offers new insights into HDL structure, composition and remodeling, and suggests that the HDL-C/ApoA-I ratio could be a readily available biomarker for estimating HDL size and HDL-P.

Corresponding Author: Norman A. Mazer, M.D., Ph.D., F. Hoffmann – La Roche, Ltd., Bldg. 670/Room 309.5, 4070 Basel, Switzerland, Tel. 011-41-61-687-9210, norman.mazer@roche.com.
Author for Reprint Requests: Samia Mora, M.D., Brigham and Women's Hospital, 900 Commonwealth Ave E, Third Floor, Boston, MA 02215. Tel. 1-617-278-0783, smora@partners.org

Previous Presentations: Preliminary versions of this work were presented orally at the KinMet Symposium, Chicago, April 27, 2011 and in poster format at the 79th European Atherosclerosis Society Congress, Gothenburg, Sweden, June 26–29, 2011 (Mazer NA and Mora S. Comparison of Theoretical and Experimental Relationships Between HDL Size and the Ratio of HDL Cholesterol (HDL-C) to Apolipoprotein A-I (ApoA-I) [Abstract]. Atherosclerosis Supplements 2011;12 (1):43).

Disclosures/Conflicts of Interest: N.A.M and P.J. are employees of F. Hoffman-La Roche, Ltd., developer of medicines intended for the treatment of cardiovascular disease; F.G. and N.P.P. report no conflicts of interest; S.M. is a consultant to Pfizer and Quest Diagnostics, and has received grant support from Astra Zeneca and Merck. Her research is supported by the NHLBI (K08 HL094375). The Women's Health Study is supported by grants HL-43851 and CA-47988 from the NHLBI and NCI.

Keywords

HDL size; HDL composition; HDL structure; Apolipoprotein; CETP; mathematical model

INTRODUCTION

Alpha high-density lipoprotein (HDL) particles are spherical in shape and contain >90% of the plasma concentrations of HDL cholesterol (HDL-C) and apolipoprotein A-I (ApoA-I) (1–3), their major protein constituent (4). They are heterogeneous in size and composition with a number of discrete HDL subclasses identified by different separation and analysis methods (5–7). The subclasses result from HDL remodeling mechanisms that involve particle fusion, lipid transfer, lipolysis and esterification (2, 3, 8) and typically range in size from about 7.5 to 11.5 nm (5–7). Collectively, alpha HDL particles are believed to play an important role in reverse cholesterol transport and in other processes that may protect individuals from cardiovascular disease (CVD) (2, 9). Current methods for determining HDL size require advanced lipoprotein testing and are not yet routinely used for clinical evaluation (5, 10). Despite considerable progress, the interrelationships between HDL size, composition and function remain incompletely understood.

In 1977 Shen *et al*. (11) proposed a simple quantitative model of lipoprotein structure based on an analysis of the size and composition of alpha HDL, LDL, VLDL, and chylomicron particles. According to their model, these lipoproteins and their subclasses have a spherical lipid core containing cholesterol esters and triglycerides, covered by a surface monolayer of phospholipids, unesterified cholesterol and apolipoprotein. The lipid core radius varies among lipoproteins; while the monolayer thickness is approximately constant and equal to 20.2 Å (11). Shen's elegant model used geometric and thermodynamic concepts to link lipoprotein size and composition. While the qualitative aspects of this model have been generally accepted, the quantitative aspects have not been fully examined, particularly in regard to HDL.

In the present study we updated Shen's model to investigate the theoretical relationship between HDL size and the corresponding ratio of HDL-C-to-ApoA-I concentrations. A mathematical derivation of the updated model and its predictions is given in the Supplemental Data to this article. The primary objective of our study is to compare these theoretical predictions with experimental data on the relationship between HDL size (determined by nuclear magnetic resonance (NMR) spectroscopy (12)) and HDL-C/ApoA-I ratio, as observed in the Women's Health Study (WHS) (13). A secondary objective is to obtain a simple equation for estimating HDL size from the HDL-C/ApoA-I ratio based on a linear regression analysis of the WHS data. We have assessed the validity of this equation by comparing its predictions with data on HDL size from patients with CETP deficiency or treated with CETP inhibitors. Lastly we show how HDL size can be combined with ApoA-I concentrations to estimate the concentration of HDL particles (HDL-P), and briefly discuss the relevance of HDL size and particle concentration as biomarkers of cardiovascular disease and diabetes.

METHODS

Update of Shen's Model

Shen's model was updated to investigate the theoretical relationship between HDL size and the HDL-C/ApoA-I ratio and to provide estimates of HDL-P. Details are provided in the Supplemental Data. Non-linear algebraic equations from the updated Shen model were programmed and solved using the Berkeley-Madonna program version 8.3.18 (http://

www.berkeleymadonna.com); tabular output was exported to Microsoft Excel 2010 for graphical representation.

WHS Population

Study participants were drawn from the WHS, a randomized, double-blind, placebo-controlled trial of low-dose aspirin and vitamin E in the primary prevention of CVD and cancer in women (13). At the time of enrollment, 28,345 subjects gave written informed consent and provided a baseline blood sample. Of these, 98.5% (n=27,909) had lipoprotein particle analysis. Subjects with missing (n=222) or anomalous (n=4) baseline data on HDL-C and/or ApoA-I, those taking lipid lowering treatments (n=891) or whose medication status was unknown (n=20) were excluded, leaving a total of 26,772 for the present analysis. The study was approved by the Institutional Review Board of the Brigham and Women's Hospital.

Laboratory Measurements

As reported previously (13), baseline EDTA plasma samples were shipped under dry ice to LipoScience Inc. (Raleigh, North Carolina) for analysis by proton NMR spectroscopy. The measured HDL diameter ($d_{avg,\ NMR}$) is an average of the calibrated diameters of individual HDL subclasses that contribute to the NMR spectra, weighted by their respective methyl NMR signals (7, 12). The $d_{avg,\ NMR}$ values are reported to a precision of 0.1 nm (by rounding); the estimated measurement coefficient of variation (CV) is 0.6% (12). The NMR method also provides a measure of the total HDL-P; CV <1.5% (12). In the current implementation of the NMR method 26 subclasses are used to determine the average HDL size and the total HDL-P (5, 12).

Baseline plasma samples were further assayed for HDL-C (mg/dL) using a direct enzymatic colorimetric assay (Roche Diagnostics; Hitachi 917 analyzer; CV <3%) (14) and for ApoA-I (mg/dL) by an immunoturbidimetric assay (DiaSorin, Stillwater, Minnesota; CV = 3%) (N. Rifai, Clinical Chemistry Laboratory, Children's Hospital, Boston, Massachusetts).

The HDL-C/ApoA-I ratio was computed from the respective mass concentrations. From the CVs and expected correlation between the HDL-C and ApoA-I concentrations, the measurement CV of the HDL-C/ApoA-I ratio is estimated to be approximately 2 – 4 %.

Statistical Analysis and Graphical Display of WHS Data

Descriptive statistics of $d_{avg,\ NMR}$, HDL-C, ApoA-I and HDL-C/ApoA-I ratio were computed on the entire WHS population along with the Pearson product-moment correlation matrix and the partial correlation matrix. As a consequence of rounding to the nearest 0.1 nm, $d_{avg,\ NMR}$ becomes a discrete variable; whereas the HDL-C/ApoA-I ratio is a continuous variable. For each discrete value of $d_{avg,\ NMR}$, the mean, SD, SEM, CV, median and interquartile range (IQR) of the HDL-C/ApoA-I ratios were computed. Linear regression was performed with HDL-C/ApoA-I (X-variable) as the dependent variable and $d_{avg,\ NMR}$ (Y-variable) as the independent variable. This approach corresponds to an "errors in variables" regression in the limit where the measurement error in the X-variable is much greater than the measurement error in the Y-variable (15), consistent with our estimates of the measurement CVs for the HDL-C/ApoA-I ratios and $d_{avg,\ NMR}$ values. The slope and intercept of the X vs. Y regression line were then transformed to express the relationship as Y vs. X. The experimental relationship between $d_{avg,\ NMR}$ vs. the HDL-C/ApoA-I ratio was displayed graphically using a combination scatter plot/heat map. The heat map divides the plot region into a grid of rectangles (width 0.025; height 0.1 nm) that are assigned a color on a white-to-red gradient based on the number of individual data points they contain.

Statistical analyses were done using R version 2.10.0 (R Foundation for Statistical Computing, Vienna, Austria).

Estimation of HDL Size in States of CETP Deficiency and Inhibition

Clinical data on HDL-C, ApoA-I and HDL size (where available) in subjects with CETP deficiency and during pharmacological inhibition of CETP activity with torcetrapib, dalcetrapib and anacetrapib were taken from the literature (16–19)*. The HDL-C/ApoA-I ratio was derived from the mean values of HDL-C and ApoA-I reported in these studies and the apparent HDL diameter was computed using the linear regression equation derived from the WHS data. It can be shown that the HDL-C/ApoA-I ratio and the HDL size computed in this way correspond to average values, weighted by the ApoA-I levels of each subject.

RESULTS

Theoretical Relationship between HDL Size and HDL-C/ApoA-I Ratio

As derived in the Supplemental Data (sections 1 and 2), the updated Shen model predicts that for a homogenous system of HDL particles with fixed values of the lipid core ratio (TG/CE_{core}) and ApoA-I fraction in the HDL proteome (F_{ApoA-I}), the particle diameter (d) will increase in a quasi-linear (monotonic) manner with the HDL-C/ApoA-I ratio. By allowing TG/CE_{core} and F_{ApoA-I} to vary over the relevant physiological ranges, a family of curves describing the theoretical relationship between d and HDL-C/ApoA-I is generated (Supplemental Data, Fig. S4). We further show in Supplemental Data (section 3) that for a heterogeneous system of HDL particles corresponding to five HDL subclasses detected by NMR spectroscopy (7), the average HDL diameter determined by NMR ($d_{avg, NMR}$) will be 5% larger on average than the diameter for the homogenous case with the same HDL-C/ApoA-I ratio (Figure S5). For this reason the theoretical curves derived for the homogeneous system should provide a reasonable prediction of the dependence of $d_{avg, NMR}$ on HDL-C/ApoA-I ratio. Lastly in Supplemental Data (section 4), we extend the concept of the HDL-C/ApoA-I ratio to the HDL-C/(ApoA-I + ApoA-II) ratio, previously used by Brinton and colleagues (20) as a surrogate for HDL size.

Experimental Relationship between HDL Size and HDL-C/ApoA-I Ratio

For the WHS population (n=26,772), the mean±SD values of the measured variables were: $d_{avg, NMR}$ (9.02±0.47 nm), HDL-C (53.9±15.0 mg/dL), ApoA-I (150.9±25.5 mg/dL) and HDL-C/ApoA-I ratio (0.354±0.063). The Pearson product-moment correlation matrix (Table 1A) shows that all of these variables are highly correlated with each other. The partial correlation matrix (Table 1B), which corrects for the inter-correlations among the variables, indicates that the strongest direct correlates of $d_{avg, NMR}$ are the HDL-C/ApoA-I ratio and ApoA-I concentration; whereas the partial correlation coefficient between $d_{avg, NMR}$ and HDL-C is not significantly different from zero.

Descriptive statistics for the HDL-C/ApoA-I ratios corresponding to each discrete value of $d_{avg, NMR}$ are given in Table 2. As $d_{avg, NMR}$ increases over the observed range (8.0 to 10.8 nm), the median (and mean) HDL-C/ApoA-I ratio increases nearly two-fold from 0.267 to 0.523; the corresponding CV values of the HDL-C/ApoA-I ratios vary between 9.6 and 16%.

*In reference 18, NMR lipoprotein profiles were reported in terms of the concentrations of small, medium and large HDL particles. The corresponding average HDL sizes obtained in that study were kindly provided to the authors by Dr. David Kallend, from data on file at F. Hoffmann-La Roche Ltd.

Fig. 1 provides a graphical representation of the experimental relationship between the HDL diameter ($d_{avg, NMR}$) and HDL-C/ApoA-I ratio in the 26,772 WHS subjects using a combination scatter plot/heat map. Individual data points in the scatter plot fall on parallel horizontal lines, corresponding to $d_{avg, NMR}$ values of 8.0, 8.1, 8.2, …, 10.8 nm. Since many data points overlap, a heat map was used to indicate the density of data points in small rectangular regions of the scatter plot. The "hottest" region, i.e., greatest density of points, corresponds to the pink/red "cigar shape" within the larger "cloud" of data points and exhibits a positive slope. The median HDL-C/ApoA-I ratios and inter-quartile ranges (IQR) for data points with the same value of $d_{avg, NMR}$ (Table 2), indicated by the diamonds and horizontal line segments, fall within the "cigar shape" region of the heat map and extend into the "cooler" region where $d_{avg, NMR}$ exceeds 10.1 nm. The least squares regression line of the HDL-C/ApoA-I ratios vs. $d_{avg, NMR}$, also shown in Fig. 1, is discussed later.

Comparison of Theoretical and Experimental Relationships between HDL Size and HDL-C/ApoA-I Ratio

Fig. 2 superimposes the family of theoretical curves derived from the updated Shen model (Supplemental Data, Fig. S4) onto the scatter plot/heat map shown in Fig. 1. For the literature-based ranges of the parameters TG/CE_{core} (0 – 0.4) and F_{ApoA-I} (50 – 90%) used in the model calculations, the theoretical curves are in reasonable quantitative agreement with the WHS data, yielding comparable sizes and bracketing the "cigar shape" region of the heat map. The two curves defined by the parameter sets $TG/CE_{core} = 0$; $F_{ApoA-I} = 70\%$ and $TG/CE_{core} = 0.133$; $F_{ApoA-I} = 60\%$ lie closest to the center of the "cigar shape" region and have a similar orientation. Theoretical curves with higher values of TG/CE_{core} (>0.2) or F_{ApoA-I} (>70%) are shifted to the left of the "cigar-shape" region; while curves with a lower value of F_{ApoA-I} (50%) are shifted to the right. It should be appreciated that the theoretical curves shown in Fig. 2 were derived independently of the WHS data, with parameter values thatwere taken from the literature, rather than estimated by curve fitting (see Supplemental Data, Table S1).

Use of Regression Equation to Estimate HDL Size from the HDL-C/ApoA-I Ratio in States of CETP Deficiency and Pharmacological Inhibition

In contrast to the theoretical curves, the least squares regression line shown in Fig. 1 was empirically derived by fitting the WHS data. It passes closely to the median HDL-C/ApoA-I values within the "cigar-shape" region, deviating slightly to the left at HDL sizes above 10.3 nm, where the data are sparse. The intercept and slope of the regression line are given in Eq. 1:

$$d_{WHS}\,(\mathrm{nm}) = 4.66 + 12.31\,\mathrm{HDL{-}C/ApoA{-}I} \quad (n = 26,772; r = 0.608) \qquad \text{Eq. 1}$$

The validity of Eq. 1 for estimating HDL size was assessed using published data from studies of subjects with homozygous and heterozygous CETP deficiency (16) and dyslipidemic subjects treated with the CETP inhibitors torcetrapib (17), dalcetrapib (18) and anacetrapib (19). Table 3 gives the mean values of HDL-C and ApoA-I in the respective subject groups, the calculated HDL-C/ApoA-I ratio, the estimated HDL size from Eq. 1 (d_{WHS}) and the measured mean HDL size (d_{meas}).

For subjects with homozygous and heterozygous CETP deficiency (16), the calculated HDL-C/ApoA-I ratios were 0.827 and 0.541, respectively, and the corresponding d_{WHS} values were 14.8 and 11.3 nm, in excellent agreement with the d_{meas} values obtained by Gel Permeation Chromatography, i.e., 14.5±1.0 and 11.8±0.6 nm. For the normal controls the

HDL-C/ApoA-I ratio was 0.355 and d_{WHS} was 9.0 nm, somewhat smaller than the measured value, 10.5±0.1 nm (16).

For dyslipidemic subjects treated with the CETP inhibitors torcetrapib (17) and dalcetrapib (18) the calculated HDL-C/ApoA-I ratios were consistent between studies and showed the expected dose-response for dalcetrapib (Table 3). Moreover the predicted d_{WHS} values were in very close agreement with the d_{meas} values obtained by NMR. For the more potent CETP inhibitor anacetrapib, the calculated HDL-C/ApoA-I ratio was 0.504 after treatment vs. 0.284 at baseline and the corresponding d_{WHS} values were 10.9 and 8.2 nm. Although HDL size was not measured in this long-term safety study (19), a recent short-term study (21) reported changes in the HDL size distribution that were qualitatively consistent with our prediction.

Estimation of HDL Particle Concentration Using the Updated Shen Model

Based on the NMR method (7, 12), the mean±SD value of the measured HDL-P in the WHS population was 35.4±6.3 umole/L. As outlined in the Supplemental Material (section 5), the updated Shen model also provides an estimate of HDL-P in each subject from the HDL size (derived from Eq. 1) and the measured ApoA-I concentration. With this approach the estimated HDL-P in the WHS population averaged 15.6±2.8 umole/L. Although the estimated and measured HDL-P concentrations differ significantly ($p<2.2\times10^{-16}$), they correlate closely on an individual basis as shown in Figure 3 and are described by the following regression equation:

$$\mathrm{HDL{-}P_{estimated}\ (umole/L)} = 4.77 + 0.307 \times \mathrm{HDL{-}P_{measured}} \quad (r=0.676) \quad \text{Eq. 2}$$

We have explored the disparity between the two measures by computing the apparent number of ApoA-I molecules per HDL particle from the ApoA-I/HDL-P ratio, using the measured and estimated HDL-P values in each subject. With the measured HDL-P the apparent number of ApoA-I molecules per HDL particle averaged 1.5±0.2 and with the estimated HDL-P it averaged 3.5±0.4 ($p<2.2\times10^{-16}$). As discussed later, the latter value is more consistent with the literature on HDL structure and composition. Further graphical analysis of these findings is presented in the Supplemental data (section 5).

DISCUSSION

Biophysical Basis of the Relationship between HDL Size and HDL-C/ApoA-I Ratio

The quasi-linear relationship between HDL size and the HDL-C/ApoA-I ratio predicted in the updated Shen model and observed in the WHS data (Fig. 1 and 2) is related to the well-known inverse relationship between the size and density of spherical lipoproteins (23). The latter derives from the fact that the lower density lipid components (CE and TG) are located within the spherical core of the particle while the higher density apolipoproteins are located on the particle surface. Based on such considerations Brinton et al. (20) used the HDL-C/(ApoA-I + ApoA-II) ratio as a surrogate for HDL size (see derivation in Supplemental Data, section 4). Similarly Miller (24, 25) used the HDL-C/ApoA-I ratio and noted its connection to the distribution of HDL2 and HDL3 particles; while Fournier reported a strong inverse relationship between triglyceride levels and the HDL-C/ApoA-I ratio (26). Most recently Kimak (27) reported a lower HDL-C/ApoA-I ratio in post-renal transplant patients indicative of smaller particles.

The updated Shen model predicts that the apolipoprotein content of an HDL particle will be approximately proportional to the radius of its lipid core rather than its surface area (Supplemental Data, Fig. S2E). This important prediction results from the curvature of the

surface monolayer and the assumption that the apolipoproteins cover the unesterified cholesterol molecules and other hydrophobic area exposed between the polar head groups of the phospholipid molecules (11). While admittedly an oversimplification of the complex interactions between apolipoproteins, unesterified cholesterol, and phospholipids, the close correspondence between the predictions of the updated Shen model with the number of ApoA-I molecules per particle in HDL subclasses reported by Kontush and Chapman (28) (Supplemental Data, Fig. S3) and with Duverger's analysis of ApoA-I-containing HDL particles (29) (Supplemental Data, Fig. S2) provide strong support for the underlying assumptions of the Shen model. The recently developed model of spherical HDL structure and ApoA-I conformational state by Davidson and colleagues (30) and the molecular dynamics simulation of spherical HDL by Vuorela (31) further refine these concepts.

Potential Relevance of the Updated Shen Model to HDL Remodeling

HDL remodeling processes such as particle fusion, lipid transfer, lipolysis and esterification (8, 9) alter the size and composition of HDL particles by adding or removing molecules from the lipid core and surface monolayer of the particles. The relationship between particle size and composition given in the updated Shen model may explain some key experimental findings in HDL remodeling, e.g., the in vitro observation that PLTP-induced fusion of small HDL particles into large HDL particles generates lipid-poor ApoA-I molecules in the medium (8). Assuming that the small particles have a diameter of 8 nm and contain 3 ApoA-I molecules, the updated Shen model predicts that fusion of two small particles will create a large particle of approximately 9 nm containing about 4 ApoA-I molecules (Supplemental Data, Fig. S3). To be compatible with the predicted surface composition, the fusion particle must release 2 ApoA-I molecules and small amounts of phospholipid and cholesterol. Such behavior has been postulated to occur in vivo as a pathway for pre-beta1 formation and is thought to be important in the process of reverse cholesterol transport (1–3, 8). Similar considerations may apply to other remodeling mechanisms (32).

Potential Use of the HDL-C/ApoA-I Ratio for Estimating HDL Size

We have shown in the case of CETP deficient populations and subjects treated with CETP inhibitors that the HDL-C/ApoA-I ratio, in conjunction with Eq. 1, provides an alternative approach for determining average HDL size. The merits of this approach include the relative ease and availability of measuring HDL-C and ApoA-I and the straightforward calculation. The downside relates to measurement error in these variables, and the fact that the relationship between HDL size and HDL-C/ApoA-I ratio also depends on other compositional variables, e.g., $F_{ApoA\text{-}I}$ and TG/CE_{core} (Fig. 2). Based on the measurement CVs of the standardized HDL-C and ApoA-I assays used in the present study, e.g., ≤3%, the variation in HDL size predicted from Eq. 1 is estimated to be ± 0.1 to 0.2 nm. From the "cigar-shape" region of the heat map, the variation in HDL size corresponding to a given HDL-C/ApoA-I ratio is approximately ± 0.4 nm, presumably due to the variation in $F_{ApoA\text{-}I}$ and TG/CE_{core}. Use of Brinton's ratio (20), HDL-C/(ApoA-I + ApoA-II), would be expected to decrease some of this variability (see Supplemental Data, section 4).

Potential Limitations of the Present Study

A potential limitation of this study is its focus on average HDL size, rather than on HDL subclasses. In principle the updated Shen model can represent the relationship between size and composition of each HDL subclass, as we have done to simulate the effects of polydispersity on the relationship between $d_{avg,\ NMR}$ and HDL-C/ApoA-I (Supplemental Data, section 3). While these effects are expected to be small, examinations of the relationship between HDL size and HDL-C/ApoA-I ratio could be performed on fractionated HDL subclasses directly. Moreover the relevance of "average HDL size" as a biomarker of HDL metabolism, pathophysiology and/or treatment-response remains to be

investigated in future experimental and theoretical studies. From the experimental perspective, a limitation of the NMR spectroscopy method is that it only provides an indirect measure of HDL size, calibrated by gradient gel electrophoresis (5, 7, 12, 33). Exploration of the updated Shen model using more direct methods for measuring HDL size would be valuable (5, 21, 34). Lastly it should be noted that data on TG/CE_{core}, $F_{ApoA\text{-}I}$ and ApoA-II were not available in the WHS study (13) to investigate the influence of these variables on HDL size.

A New Approach for Estimating HDL Particle Concentration

We have shown how one may use the HDL size (inferred from the HDL-C/ApoA-I ratio) and ApoA-I concentration to estimate HDL-P. The values of HDL-P obtained in this manner correlate with the NMR measurements of total HDL-P but are approximately 50–60% lower. Using the HDL-P values obtained by both approaches we have calculated the apparent number of ApoA-I molecules per HDL particle and find that our new approach provides a result that is more concordant with literature values (28) for the number of ApoA-I molecules contained in HDL particles of different sizes (Supplemental Data, Fig. S6). Further studies are needed to confirm this finding and reassess the predictive value of the estimated HDL-P values to cardiovascular risk, as recently reported for HDL-P values obtained by NMR in the MESA study (22).

Relationship between HDL-C/ApoA-I Ratio and HDL Size to CVD Risk

Miller et al (24, 25) previously reported that the HDL-C/ApoA-I ratio was lower in patients with coronary heart disease compared to controls, suggesting that smaller average HDL size may be associated with greater CVD risk. In a previous analysis of the WHS study (13) lower HDL size (measured by NMR) was also associated with greater CVD risk. In contrast, van der Steeg et al. (35) suggested that after controlling for ApoA-I and Apo-B levels, CVD risk in the EPIC study may actually increase with larger HDL size. In a later analysis of the EPIC study, Arsenault et al. (36) found no adverse effect of large HDL size after controlling for standard CVD risk factors (including diabetes) and HDL-C levels. In recent analyses of the WHS study, average HDL size was found to be a stronger independent predictor of incident hypertension and diabetes than HDL-C (37, 38). Further research is needed to clarify the precise relationship between HDL size and CVD risk. In the absence of HDL size measurements, the HDL-C/ApoA-I ratio may be a useful surrogate biomarker for HDL size or used to estimate HDL size by Eq. 1.

Supplementary Material

Refer to Web version on PubMed Central for supplementary material.

Acknowledgments

The authors would like to collectively thank many individuals for helpful feedback on earlier versions of this work that were presented at the KinMet Symposium (April 2011, Chicago) and the 79th Congress of the European Atherosclerosis Society (June 2011, Gothenburg). Particular thanks are expressed to Dr. Betty Shen, Fred Hutchinson Cancer Research Center, for helpful correspondence on her 1977 paper and to Dr. Nicolas Frey and Dr. James Lu of Hoffman-LaRoche Ltd., for their insightful comments on the manuscript.

List of Abbreviations

HDL	high-density lipoprotein
ApoA-I	apolipoprotein A-I

ApoA-II	apolipoprotein A-II
C	cholesterol
CE	cholesterol ester
TG	triglyceride
CETP	cholesterol ester transfer protein
PLTP	phospholipid transfer protein
LDL	low-density lipoprotein
VLDL	very low-density lipoprotein
CVD	cardiovascular disease
CV	coefficient of variation
NMR	nuclear magnetic resonance
WHS	Women's Health Study

References

1. O'Connor PM, Naya-Vigne JM, Duchateau PN, Ishida BY, Mazur M, Schoenhaus SA, Zysow BR, et al. Measurement of prebeta-1 HDL in human plasma by an ultrafiltration-isotope dilution technique. Anal Biochem. 1997; 251(2):234–40. [PubMed: 9299021]
2. Barter, PJ.; Clay, MA.; Rye, KA. Chapter 5: High Density Lipoproteins: The Anti-atherogenic Fraction. In: Barter, PJ.; Rye, KA., editors. Plasma Lipids and Their Role in Disease. Amsterdam: Harwood Academic Publishers; 1999. p. 85-107.
3. Kunitake ST, Mendel CM, Hennessy LK. Interconversion between apolipoprotein A-I-containing lipoproteins of pre-beta and alpha electrophoretic mobilities. J Lipid Res. 1992; 33(12):1807–16. [PubMed: 1479290]
4. Vaisar T, Pennathur S, Green PS, Gharib SA, Hoofnagle AN, Cheung MC, Byun J, et al. Shotgun proteomics implicates protease inhibition and complement activation in the antiinflammatory properties of HDL. J Clin Invest. 2007; 117(3):746–56. [PubMed: 17332893]
5. Rosenson RS, Brewer HB Jr, Chapman MJ, Fazio S, Hussain MM, Kontush A, Krauss RM, et al. HDL measures, particle heterogeneity, proposed nomenclature, and relation to atherosclerotic cardiovascular events. Clin Chem. 2011; 57(3):392–410. [PubMed: 21266551]
6. Blanche PJ, Gong EL, Forte TM, Nichols AV. Characterization of human high-density lipoproteins by gradient gel electrophoresis. Biochim Biophys Acta. 1981; 665(3):408–19. [PubMed: 7295744]
7. Otvos JD. Measurement of lipoprotein subclass profiles by nuclear magnetic resonance spectroscopy. Clin Lab. 2002; 48(3–4):171–80. [PubMed: 11934219]
8. Rye KA, Clay MA, Barter PJ. Remodelling of high density lipoproteins by plasma factors. Atherosclerosis. 1999; 145(2):227–38. [PubMed: 10488948]
9. Brewer HB Jr. Clinical review: The evolving role of HDL in the treatment of high-risk patients with cardiovascular disease. J Clin Endocrinol Metab. 2011; 96(5):1246–57. [PubMed: 21389140]
10. Mora S. Advanced lipoprotein testing and subfractionation are not (yet) ready for routine clinical use. Circulation. 2009; 119(17):2396–404. [PubMed: 19414657]
11. Shen BW, Scanu AM, Kézdy FJ. Structure of human serum lipoproteins inferred from compositional analysis. Proc Natl Acad Sci U S A. 1977; 74(3):837–41. [PubMed: 265578]
12. Jeyarajah EJ, Cromwell WC, Otvos JD. Lipoprotein particle analysis by nuclear magnetic resonance spectroscopy. Clin Lab Med. 2006; 26(4):847–70. [PubMed: 17110242]
13. Mora S, Otvos JD, Rifai N, Rosenson RS, Buring JE, Ridker PM. Lipoprotein particle profiles by nuclear magnetic resonance compared with standard lipids and apolipoproteins in predicting incident cardiovascular disease in women. Circulation. 2009; 119(7):931–9. [PubMed: 19204302]

14. Sugiuchi H, Uji Y, Okabe H, Irie T, Uekama K, Kayahara N, Miyauchi K. Direct measurement of high-density lipoprotein cholesterol in serum with polyethylene glycol-modified enzymes and sulfated alpha-cyclodextrin. Clin Chem. 1995; 41(5):717–23. [PubMed: 7729051]
15. Casella G, Berger RL. Statistical Inference. Pacific Grove: Wadsworth & Brooks/Cole Advanced Books & Software. 1990:581–594.
16. Yamashita S, Hui DY, Wetterau JR, Sprecher DL, Harmony JA, Sakai N, Matsuzawa Y, et al. Characterization of plasma lipoproteins in patients heterozygous for human plasma cholesteryl ester transfer protein (CETP) deficiency: plasma CETP regulates high-density lipoprotein concentration and composition. Metabolism. 1991; 40(7):756–63. [PubMed: 1870431]
17. Brousseau ME, Schaefer EJ, Wolfe ML, Bloedon LT, Digenio AG, Clark RW, Mancuso JP, et al. Effects of an inhibitor of cholesteryl ester transfer protein on HDL cholesterol. N Engl J Med. 2004; 350(15):1505–15. [PubMed: 15071125]
18. Ballantyne CM, Miller M, Niesor EJ, Burgess T, Kallend D, Stein EA. Effect of dalcetrapib plus pravastatin on lipoprotein metabolism and high-density lipoprotein composition and function in dyslipidemic patients: results of a phase IIb dose-ranging study. Am Heart J. 2012 Mar; 163(3): 515–21. 521.e1–3. [PubMed: 22424025]
19. Cannon CP, Shah S, Dansky HM, Davidson M, Brinton EA, Gotto AM, Stepanavage M, et al. Safety of anacetrapib in patients with or at high risk for coronary heart disease. N Engl J Med. 2010; 363(25):2406–15. [PubMed: 21082868]
20. Brinton EA, Eisenberg S, Breslow JL. Human HDL cholesterol levels are determined by apoA-I fractional catabolic rate, which correlates inversely with estimates of HDL particle size. Effects of gender, hepatic and lipoprotein lipases, triglyceride and insulin levels, and body fat distribution. Arterioscler Thromb. 1994; 14(5):707–20. [PubMed: 8172849]
21. Krauss RM, Wojnooski K, Orr J, Geaney JC, Pinto CA, Liu Y, Wagner JA, et al. Changes in lipoprotein subfraction concentration and composition in healthy individuals treated with the CETP inhibitor anacetrapib. J Lipid Res. 2012; 53(3):540–7. [PubMed: 22180633]
22. Mackey RH, Greenland P, Goff DC Jr, Lloyd-Jones D, Sibley CT, Mora S. High-density lipoprotein cholesterol and particle concentrations, carotid atherosclerosis, and coronary events: MESA (multi-ethnic study of atherosclerosis). J Am Coll Cardiol. 2012; 60(6):508–16. [PubMed: 22796256]
23. Scanu, AM.; Kruski, AW. Chapter 2: The Chemistry of Serum Lipoproteins. In: Abraham, S., editor. Pharmacology of Lipid transport and Atherosclerotic Processes (International Encyclopedia of Pharmacology and Therapeutics, section 24). Oxford: Pergamon Press Ltd; 1975. p. 21-38.
24. Miller NE. Associations of high-density lipoprotein subclasses and apolipoproteins with ischemic heart disease and coronary atherosclerosis. Am Heart J. 1987; 113(2 Pt 2):589–97. [PubMed: 3544775]
25. Miller NE, Rajput-Williams J, Nanjee MN, Samuel L, Albers JJ. Relationship of high density lipoprotein composition to plasma lecithin:cholesterol acyltransferase concentration in men. Atherosclerosis. 1988; 69(2–3):123–9. [PubMed: 3126747]
26. Fournier N, Atger V, Cogny A, Vedie B, Giral P, Simon A, Moatti N, et al. Analysis of the relationship between triglyceridemia and HDL-phospholipid concentrations: consequences on the efflux capacity of serum in the Fu5AH system. Atherosclerosis. 2001; 157(2):315–23. [PubMed: 11472731]
27. Kimak E, Hałabiś M, Baranowicz-Gaszczyk I. Relationships between serum lipid, lipoprotein, triglyceride-rich lipoprotein, and high-density lipoprotein particle concentrations in post-renal transplant patients. J Zhejiang Univ Sci B. 2010; 11(4):249–57. [PubMed: 20349521]
28. Kontush A, Chapman MJ. Functionally defective high-density lipoprotein: a new therapeutic target at the crossroads of dyslipidemia, inflammation, and atherosclerosis. Pharmacol Rev. 2006; 58(3): 342–74. [PubMed: 16968945]
29. Duverger N, Rader D, Duchateau P, Fruchart JC, Castro G, Brewer HB Jr. Biochemical characterization of the three major subclasses of lipoprotein A-I preparatively isolated from human plasma. Biochemistry. 1993; 32(46):12372–9. [PubMed: 8241125]

30. Huang R, Silva RA, Jerome WG, Kontush A, Chapman MJ, Curtiss LK, Hodges TJ, et al. Apolipoprotein A-I structural organization in high-density lipoproteins isolated from human plasma. Nat Struct Mol Biol. 2011; 18(4):416–22. [PubMed: 21399642]

31. Vuorela T, Catte A, Niemelä PS, Hall A, Hyvönen MT, Marrink SJ, Karttunen M, et al. Role of lipids in spheroidal high density lipoproteins. PLoS Comput Biol. 2010; 6(10):e1000964. [PubMed: 21060857]

32. Niesor EJ. Different effects of compounds decreasing cholesteryl ester transfer protein activity on lipoprotein metabolism. Curr Opin Lipidol. 2011; 22(4):288–95. [PubMed: 21587074]

33. Grundy SM, Vega GL, Otvos JD, Rainwater DL, Cohen JC. Hepatic lipase activity influences high density lipoprotein subclass distribution in normotriglyceridemic men. Genetic and pharmacological evidence. J Lipid Res. 1999; 40(2):229–34. [PubMed: 9925651]

34. Asztalos BF, Schaefer EJ. High-density lipoprotein subpopulations in pathologic conditions. Am J Cardiol. 2003; 91(7A):12E–17E. [PubMed: 12505564]

35. van der Steeg WA, Holme I, Boekholdt SM, Larsen ML, Lindahl C, Stroes ES, Tikkanen MJ, et al. High-density lipoprotein cholesterol, high-density lipoprotein particle size, and apolipoprotein A-I: significance for cardiovascular risk: the IDEAL and EPIC-Norfolk studies. J Am Coll Cardiol. 2008; 51(6):634–42. [PubMed: 18261682]

36. Arsenault BJ, Lemieux I, Després JP, Wareham NJ, Stroes ES, Kastelein JJ, Khaw KT, et al. Comparison between gradient gel electrophoresis and nuclear magnetic resonance spectroscopy in estimating coronary heart disease risk associated with LDL and HDL particle size. Clin Chem. 2010; 56(5):789–98. [PubMed: 20348400]

37. Paynter NP, Sesso HD, Conen D, Otvos JD, Mora S. Lipoprotein subclass abnormalities and incident hypertension in initially healthy women. Clin Chem. 2011; 57(8):1178–87. [PubMed: 21700954]

38. Mora S, Otvos JD, Rosenson RS, Pradhan A, Buring JE, Ridker PM. Lipoprotein particle size and concentration by nuclear magnetic resonance and incident type 2 diabetes in women. Diabetes. 2010; 59(5):1153–60. [PubMed: 20185808]

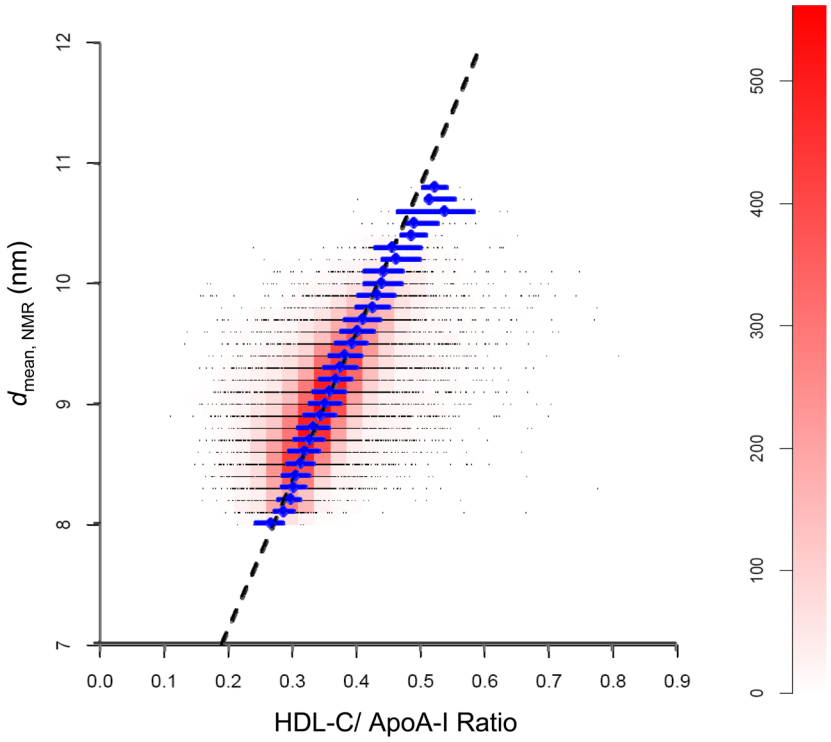

Fig. 1.

Scatter plot/heat map of the experimental relationship between the diameter of the HDL particles determined by NMR spectroscopy ($d_{avg, NMR}$) and the corresponding HDL-C/ApoA-I ratio from the WHS study (n=26,772). Data points (black dots) represent baseline values from individual subjects. Due to overlap of the points, these appear as black horizontal lines corresponding to the measured values of $d_{avg, NMR}$, e.g., 8.0, 8.1, 8.2, 8.3, etc. The color scale on the right vertical axis (heat map) indicates the number of data points within the unit rectangles (width 0.025; height 0.1 nm) that are adjacent to each other on each horizontal line. The pink/red "cigar shape" region corresponds to the highest density of data points in the WHS population. Blue diamonds represent the median HDL-C/ApoA-I ratio for data points with the same value of $d_{avg, NMR}$; horizontal blue line-segments represent the corresponding interquartile ranges. The dashed black line is based on a regression analysis of the HDL-C/ApoA-I ratios vs. the $d_{avg, NMR}$ values. The equation is given by: $d_{avg, NMR} = 4.66 + 12.31$ HDL-C/ApoA-I. See Experimental Methods (Statistical Analysis of WHS Data) for details.

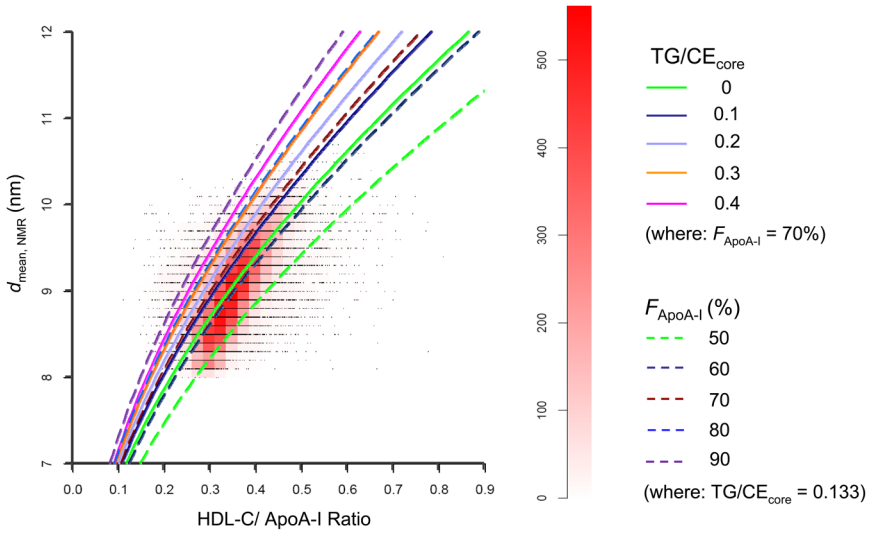

Fig. 2.

Superposition of the theoretical relationship (solid and dashed curves) between HDL diameter and HDL-C/ApoA-I ratio derived from the updated Shen model on the scatter plot/heat plot of the WHS data (Fig. 1). The theoretical curves also depend on the molar ratio of triglyceride-to-cholesterol ester in the hydrophobic core of the particles (TG/CE_{core}) and the fraction of ApoA-I in the HDL proteome (F_{ApoA-I}). See Supplemental Data for a derivation of the theoretical relationship based on the updated Shen model.

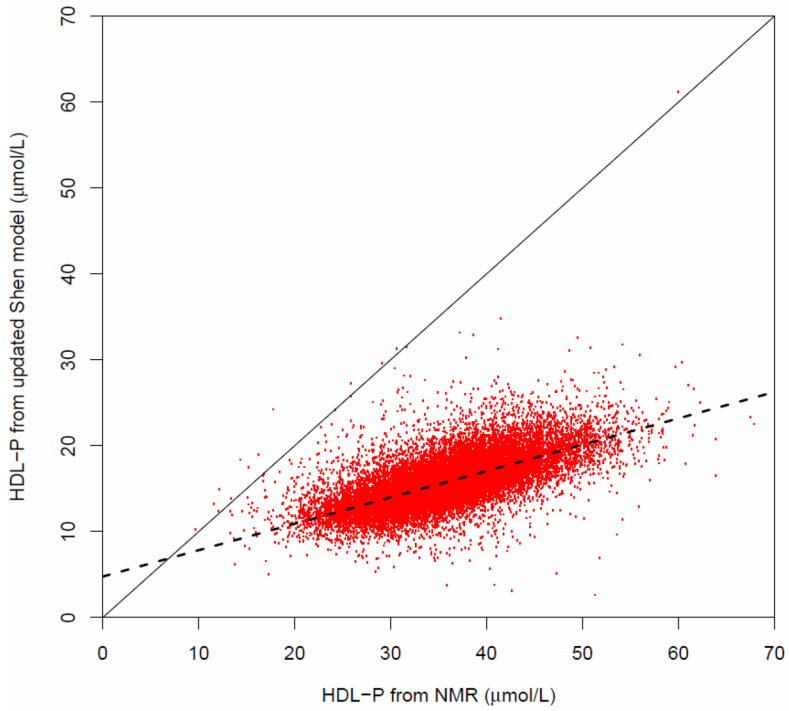

Fig. 3.

Correlation plot of the estimated HDL particle concentrations derived from the HDL-C/ApoA-I ratio and the ApoA-I concentration using the updated Shen model vs. the measured HDL particle concentrations obtained from NMR sprectroscopy in the WHS (n=26,772). Solid line corresponds to the line of identity. Dashed line corresponds to linear regression equation (Y = 4.77 + 0.307 X; r=0.676).

Table 1A

Pearson product-moment correlation matrix (r-values) *

	HDL-C	ApoA-I	HDL-C/ApoA-I
$d_{avg, NMR}$	0.738	0.577	0.608
HDL-C		0.779	0.801
ApoA-I			0.269

*Note: all r-values and partial correlations are highly significant ($P<2.2 \times 10^{-16}$), except for the partial correlation between $d_{avg, NMR}$ and HDL-C (P=0.981)

Table 1B

Partial correlation matrix *

	HDL-C	ApoA-I	HDL-C/ApoA-I
$d_{avg, NMR}$	−0.00015	0.130	0.136
HDL-C		0.971	0.972
ApoA-I			−0.950

*Note: all r-values and partial correlations are highly significant ($P<2.2 \times 10^{-16}$), except for the partial correlation between $d_{avg, NMR}$ and HDL-C (P=0.981)

Table 2

Descriptive statistics and quartile analysis of HDL-C/ApoA-I ratios corresponding to each average HDL diameter measured by NMR ($d_{avg, NMR}$) in the WHS population.

$d_{avg,NMR}$ (nm)	N	Mean	SD	SEM	CV(%)	Q1(25%)	Q2(50%)	Q3(75%)
8.0	10	0.267	0.033	0.010	12.3	0.242	0.267	0.286
8.1	178	0.291	0.047	0.004	16.1	0.271	0.287	0.303
8.2	582	0.296	0.036	0.001	12.1	0.277	0.297	0.313
8.3	1085	0.303	0.041	0.001	13.4	0.282	0.302	0.321
8.4	1441	0.305	0.040	0.001	13.2	0.284	0.304	0.326
8.5	1620	0.314	0.041	0.001	13.2	0.291	0.313	0.334
8.6	1793	0.319	0.043	0.001	13.6	0.294	0.319	0.341
8.7	1884	0.326	0.046	0.001	13.9	0.302	0.327	0.350
8.8	1929	0.334	0.048	0.001	14.5	0.309	0.333	0.357
8.9	2023	0.343	0.050	0.001	14.6	0.318	0.343	0.368
9.0	1953	0.351	0.051	0.001	14.5	0.326	0.351	0.375
9.1	1991	0.358	0.050	0.001	14.0	0.332	0.358	0.383
9.2	1840	0.367	0.051	0.001	13.8	0.342	0.367	0.392
9.3	1723	0.376	0.053	0.001	14.1	0.350	0.376	0.401
9.4	1587	0.383	0.051	0.001	13.3	0.357	0.382	0.409
9.5	1318	0.394	0.053	0.001	13.5	0.368	0.394	0.417
9.6	1096	0.401	0.057	0.002	14.1	0.375	0.402	0.427
9.7	884	0.409	0.057	0.002	14.0	0.382	0.410	0.438
9.8	656	0.428	0.059	0.002	13.8	0.399	0.426	0.452
9.9	482	0.432	0.068	0.003	15.6	0.403	0.433	0.460
10.0	305	0.440	0.065	0.004	14.7	0.412	0.440	0.472
10.1	181	0.445	0.068	0.005	15.2	0.412	0.442	0.473
10.2	88	0.461	0.054	0.006	11.7	0.441	0.462	0.499
10.3	68	0.465	0.064	0.008	13.9	0.430	0.457	0.501
10.4	18	0.494	0.050	0.012	10.1	0.470	0.486	0.509
10.5	18	0.496	0.048	0.011	9.6	0.474	0.491	0.528
10.6	11	0.528	0.079	0.024	15.0	0.464	0.539	0.584
10.7	6	0.515	0.063	0.026	12.2	0.511	0.514	0.554

$d_{avg,NMR}$ (nm)	N	Mean	SD	SEM	CV(%)	Q1(25%)	Q2(50%)	Q3(75%)
10.8	2	0.523	0.053	0.038	10.2	0.504	0.523	0.542

Table 3

HDL-C, ApoA-I, HDL-C/ApoA-I ratio and HDL diameters computed with Eq. 1 (d_{WHS}) and measured (d_{meas}) in populations with CETP deficiency and/or treated with CETP Inhibitors.

Population/Treatment Regimen (n)	Ref.	HDL-C [a] (mg/dL)	ApoA-I [a] (mg/dL)	HDL-C/ApoA-I (dimensionless)	d_{WHS} (nm)	d_{meas} [a] (nm)
CETP homozygotes (n=4)	16	193 ± 28	233.5 ± 22.3	0.827	14.8	14.5 ± 1.0 [b]
CETP homozygotes (n=15)	16	84 ± 25	155.3 ± 22.1	0.541	11.3	11.8 ± 0.6 [b]
Normal Controls (n=20)	16	50 ± 8	140.9 ± 16.1	0.355	9.0	10.5 ± 0.1 [b]
Torcetrapib 120 mg BID × 4 wk (n=6)	17	70 ± 15	151 ± 6	0.464	10.4	9.7 ± 0.7 [c]
Baseline (n=6)	17	34 ± 5	112 ± 13	0.304	8.4	8.4 ± 0.4 [c]
Dalcetrapib 900 mg QD × 12 wk (n=72)	18 [d]	51.5 ± 12.5	147.2 ± 27.1	0.349	9.0	8.9 ± 0.4 [c]
Dalcetrapib 600 mg QD × 12 wk (n=67)	18 [d]	50.5 ± 10.7	149.2 ± 25.0	0.338	8.8	8.8 ± 0.4 [c]
Dalcetrapib 300 mg QD × 12 wk (n=75)	18 [d]	44.0 ± 9.4	137.7 ± 22.1	0.320	8.6	8.6 ± 0.3 [c]
Placebo (n=73)	18 [d]	39.2 ± 7.2	132.2 ± 19.1	0.296	8.3	8.4 ± 0.3 [c]
Anacetrapib 100 mg QD × 76 wk (n=541)	19	102.3	203	0.504	10.9	NR [e]
Baseline (n=797)	19	40.5	142.5	0.284	8.2	NR [e]

[a] Mean ± SD (where available).

[b] measured by Gel Permeation Chromatography (GPC);

[c] measured by NMR spectroscopy;

[d] HDL size measurements corresponding to ref. 18 were supplied by Dr. David Kallend, from data on file F. Hoffmann-LaRoche, Ltd.;

[e] NR = not reported